A First Principles Theory of Nuclear Magnetic Resonance J-Coupling in solid-state systems.

Siân A. Joyce,[1] Jonathan R. Yates,[2] Chris J. Pickard,[3] and Francesco Mauri[4]

[1]*Tyndall National Institute, Lee Maltings, Prospect Row, Cork, Ireland*
[2]*TCM Group, Cavendish Laboratory, University of Cambridge, UK*
[3]*School of Physics and Astronomy, University of St. Andrews, St. Andrews, Scotland*
[4]*Institut de Minéralogie et de Physique des Milieux Condensés, Université Pierre et Marie Curie, Paris, France*
(Dated: February 1, 2008)

A method to calculate NMR J-coupling constants from first principles in extended systems is presented. It is based on density functional theory and is formulated within a planewave-pseudopotential framework. The all-electron properties are recovered using the projector augmented wave approach. The method is validated by comparison with existing quantum chemical calculations of solution-state systems and with experimental data. The approach has been applied to verify measured J-coupling in a silicophosphate structure, $Si_5O(PO_4)_6$.

I. INTRODUCTION

Nuclear Magnetic Resonance (NMR) allows information to be relayed through magnetic nuclei in a non-destructive and powerful approach to structural elucidation. It is a fundamental tool in a broad range of scientific disciplines and is a cornerstone of modern spectroscopy. NMR spectra yield a wealth of information, the most commonly reported property being the chemical shift. This parameter relates an externally applied magnetic field to the resulting change in the local electronic environment of the magnetic nuclei, thereby providing key insight into the underlying atomic structure.

NMR J-coupling or indirect nuclear spin-spin coupling is an indirect interaction of the nuclear magnetic moments mediated by the bonding electrons. It is manifested as the fine-structure in NMR spectra, providing a direct measure of bond-strength and a map of the connectivities of the system. The J-coupling mechanism is an essential component of many NMR experiments.[1]

In solution-state, J-coupling measurements can often be obtained from one dimensional spectra where the multiplet splitting in the peaks is clearly resolved. However, in the solid-state this is not the case as these splittings are typically obscured by the broadenings from anisotropic interactions. Fortunately this technical challenge has not prevented the determination of J-coupling in the solid-state, as recent work employing spin-echo Magic Angle Spinning (MAS) techniques[2] has resulted in accurate measurements of J-coupling in both inorganic materials[3,4,5,6] and molecular crystals.[7,8,9,10,11] In combination with the advances in solid-state experiments, there has also been an increased interest from the biomolecular community as J-coupling has been found to be a direct measure of hydrogen bond strength.[11,12,13] Both of these factors have provided a strong impetus to develop first principles approaches to compute the NMR J-coupling constants in order to support experimental work, particularly for solid-state systems.

For finite systems, NMR parameters, including both chemical shifts and J-couplings, can be routinely calculated using traditional quantum chemistry approaches based on localised orbitals.[14,15] Such calculations have been widely applied to assign the solution-state NMR spectra of molecular systems and establish key conformational and structural trends.[16] In particular NMR J-couplings have been used to quantify hydrogen bonding[17] in biological systems. In order to apply these techniques to solid-state NMR, it is necessary to devise finite clusters of atoms which model the local environment around a site of interest in the true extended structure. While this has led to successful studies of NMR chemical shifts in systems such as molecular crystals,[18] supra-molecular assemblies[19] and organo-metallic compounds,[20] it is clear that there are advantages in an approach that inherently takes account of the long-range electrostatic effects in extended systems.

This observation has led to the recent development of the Gauge Including Projector Augmented Wave (GIPAW)[21] method which enables NMR parameters to be calculated at all-electron accuracy within the planewave-pseudopotential formalism[22] of density functional theory (DFT). The technique has been applied, in combination with experimental NMR spectroscopy, to systems such as minerals,[23,24,25] glasses[26,27] and molecular crystals.[28,29,30]

In this paper we introduce a theory to compute NMR J-Couplings in extended systems using periodic boundary conditions and supercells with the planewave-pseudopotential approach. Like the GIPAW approach to calculating NMR chemical shifts, our method is formulated within the planewave-pseudopotential framework using density functional perturbation theory (DFPT). We use the projector-augmented-wave[31] (PAW) reconstruction technique to calculate J-couplings with all-electron accuracy.

In the following section we discuss the physical mechanism of the indirect spin-spin interaction, the basis of the PAW approach and the supercell technique. In Sections III and IV we show how the J-coupling tensor maybe be calculated using PAW and DFPT. The method has been implemented in a parallel plane-wave electronic structure

code and we discuss details of the implementation and provide validation results in Section V.

II. NMR J-COUPLING

We consider the interaction of two nuclei, K and L, with magnetic moments, $\boldsymbol{\mu}_K$ and $\boldsymbol{\mu}_L$, mediated by the electrons. The first complete analysis of this indirect coupling was provided by Ramsey[32,33] who decomposed the interaction into four distinct physical mechanisms; two involving the interaction of the nuclear spins through the electron spin and two through the electron charge. In the absence of spin-orbit coupling i.e, for relatively light elements, the charge and spin interactions can be treated separately. We can write the magnetic field at atom L induced by the magnetic moment of atom K as

$$
\begin{aligned}
\mathbf{B}_{\text{in}}^{(1)}(\mathbf{R}_L) \;=\; & \frac{\mu_0}{4\pi} \int \left[\frac{3(\mathbf{m}^{(1)}(\mathbf{r}) \cdot \mathbf{r}_L)\mathbf{r}_L - \mathbf{m}^{(1)}(\mathbf{r})|\mathbf{r}_L|^2}{|\mathbf{r}_L|^5} \right] \, \mathrm{d}^3\mathbf{r} \\
& + \frac{\mu_0}{4\pi} \frac{8\pi}{3} \int \mathbf{m}^{(1)}(\mathbf{r})\delta(\mathbf{r}_L) \, \mathrm{d}^3\mathbf{r} \\
& + \frac{\mu_0}{4\pi} \int \mathbf{j}^{(1)}(\mathbf{r}) \times \frac{\mathbf{r}_L}{|\mathbf{r}_L|^3} \, \mathrm{d}^3\mathbf{r}.
\end{aligned}
\tag{1}
$$

$\mathbf{r}_L = \mathbf{R}_L - \mathbf{r}$, where $\mathbf{R}_L$ is the position of nucleus L, μ_0 is the permeability of a vacuum and δ is the Dirac delta function.

$\boldsymbol{\mu}_K$ interacts with the electron spin through a magnetic field generated by a Fermi-contact term, which is due to the finite probability of the presence of an electron at the nucleus, and a spin-dipolar interaction. Both of these terms give rise to a first order spin magnetisation density, $\mathbf{m}^{(1)}(\mathbf{r})$. This magnetisation density then induces a magnetic field at the receiving nucleus by the same mechanisms, which in this case are given respectively by the first and second terms of Eqn. 1. The interaction between $\boldsymbol{\mu}_K$ and the electronic charge gives rise to an induced current density. To first-order this is given by $\mathbf{j}^{(1)}(\mathbf{r})$ and can be divided into a paramagnetic and a diamagnetic contribution.

The J-coupling tensor, $\overleftrightarrow{\mathbf{J}}_{LK}$, between L and K, can be related to the induced field by

$$
\mathbf{B}_{\text{in}}^{(1)}(\mathbf{R}_L) = \frac{2\pi}{\hbar\gamma_L\gamma_K} \overleftrightarrow{\mathbf{J}}_{LK} \cdot \boldsymbol{\mu}_K,
\tag{2}
$$

where γ_L and γ_K are the gyromagnetic ratios of nuclei L and K. Although the physical interpretation of J-coupling is simplified by considering the interaction in terms of a responding and a perturbing nucleus, it is a symmetric coupling and either atom L or K can be considered as the perturbing site. Experimental interest is focused primarily on the isotropic coupling constant, J_{LK}^n, which is obtained from the trace of $\overleftrightarrow{\mathbf{J}}_{LK}$ and is measured in Hz. The superscript, n, denotes the order of the coupling in terms of the number of bonds separating the coupled nuclei. In a typical NMR experiment

J-coupling can be measured across a maximum of three bonds.[34,35] In this paper we concentrate solely on obtaining the isotropic or scalar value.

To calculate $\overleftrightarrow{\mathbf{J}}_{KL}$ we obtain $\mathbf{m}^{(1)}$ and $\mathbf{j}^{(1)}$ within density functional perturbation theory using a planewave expansion for the wavefunctions with periodic boundary conditions and pseudopotentials to represent the ionic cores. The use of pseudopotentials generates a complication as the J-coupling tensor depends critically on the wavefunction in the regions close to the perturbing and receiving nuclei, precisely the regions where the pseudo-wavefunctions have a non-physical form. To compensate for this we perform an all-electron reconstruction of the valence wavefunctions in the core region using Blöchl's projector augmented wave (PAW) scheme.[36]

Within this scheme, the expectation value of an operator O, applied to the all-electron wavefunctions, $|\psi\rangle$, is expressed in terms of the pseudised wavefunctions, $|\widetilde{\psi}\rangle$, as: $\langle\psi|O|\psi\rangle = \langle\widetilde{\psi}|\widetilde{O}|\widetilde{\psi}\rangle$. Here, for an all-electron local or semi-local operator, O, the corresponding pseudo-operator, $\widetilde{O}$, is given by

$$
\begin{aligned}
\widetilde{O} \;=\; & O + \sum_{\mathbf{R},n,m} |\widetilde{p}_{\mathbf{R},n}\rangle \, [\langle\phi_{\mathbf{R},n}|O|\phi_{\mathbf{R},m}\rangle \\
& - \langle\widetilde{\phi}_{\mathbf{R},n}|O|\widetilde{\phi}_{\mathbf{R},m}\rangle \,] \, \langle\widetilde{p}_{\mathbf{R},m}|.
\end{aligned}
\tag{3}
$$

$\mathbf{R}$ labels the atomic site, or augmentation region, and n and m are composite indexes which account for the angular momentum channels and the number of projectors. $|\phi_{\mathbf{R},n}\rangle$ are the all-electron partial waves obtained as eigenstates of an atomic calculation within r_c, the pseudopotential core radius and $|\widetilde{\phi}_{\mathbf{R},n}\rangle$ are the corresponding pseudo partial waves. $|\widetilde{p}_{\mathbf{R},n}\rangle$ are the localised projectors which weight the superposition of partial waves where $\langle\widetilde{p}_{\mathbf{R},n}|\widetilde{\phi}_{\mathbf{R}',m}\rangle = \delta_{\mathbf{R}\mathbf{R}'}\delta_{nm}$. The PAW method has been used to calculate several all-electron properties from pseudopotential calculations including: EPR hyperfine parameters,[36] electric field gradient tensors[37] and Electron Energy Loss Spectroscopy.[38]

To calculate J-couplings in the solid-state using periodic boundary conditions, the perturbing nucleus can be viewed similar to a defect in a defect calculation. This allows us to use the standard technique of constructing supercells from the unit cell which are large enough to inhibit the interaction between the periodic defects or perturbations. This corresponds to extending the system-size to facilitate the decay of the induced magnetisation and current densities within the simulation cell. Figure. 1 is a schematic of a $2 \times 2 \times 2$ supercell constructed from eight unit cells. The perturbing atom now lies at the corner of a much larger cell which decreases the interaction between the perturbation and its periodic image. This approach works very well for localised properties such as J-coupling. To calculate the J-coupling for molecules, we use a vacuum supercell technique. In both cases, the J-couplings must be converged with respect to the cell-size.
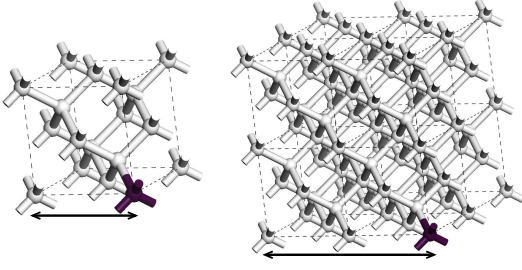
FIG. 1: Schematic of the supercell technique. The unit cell is on the left, a 2×2×2 supercell of the unit cell is on the right. This supercell doubles the distance between the perturbing atom (black) and its periodic image in the next cell.

III. THE SPIN MAGNETISATION DENSITY

We now obtain the contribution to the J-coupling tensor which arises from the interaction of the nuclear spins mediated by the electron spin. We first obtain an expression for the pseudo-Hamiltonian in the presence of a perturbing nuclear spin and show how it can be used to obtain the induced magnetisation density. We then use the magnetisation density to calculate the magnetic field induced at the receiving nucleus.

A. Pseudo-Hamiltonian

The all-electron Hamiltonian for a system containing N magnetic moments which interact through the electron spin, $\mathbf{S}$, is expanded to first order in the magnetic moment of the perturbing site, $\boldsymbol{\mu}_K$, to give

$$H = \frac{1}{2}\mathbf{p}^2 + V^{(0)}(\mathbf{r}) + V^{(1)}(\mathbf{r}) + H_{SD} + H_{FC}. \quad (4)$$

where

$$H_{SD} = g\beta\mathbf{S} \cdot \mathbf{B}_K^{SD}, \quad (5)$$

and

$$H_{FC} = g\beta\mathbf{S} \cdot \mathbf{B}_K^{FC}. \quad (6)$$

$\mathbf{B}_K^{SD}$ is the magnetic field generated by a spin-dipole interaction,

$$\mathbf{B}_K^{SD} = \frac{\mu_0}{4\pi}\frac{3\mathbf{r}_K(\mathbf{r}_K \cdot \boldsymbol{\mu}_K) - r_K^2\boldsymbol{\mu}_K\mathcal{I}}{|r_K|^5}, \quad (7)$$

and $\mathbf{B}_K^{FC}$ is the Fermi contact interaction,

$$\mathbf{B}_K^{FC} = \frac{8\pi}{3}\delta(\mathbf{r}_K)\boldsymbol{\mu}_K. \quad (8)$$

We have defined $\mathbf{r}_K = \mathbf{R}_K - \mathbf{r}$, where $\mathbf{R}_K$ is the position of nucleus K and $\mathcal{I}$ is the identity matrix. Here $V^{(0)}(\mathbf{r})$ is the ground-state all-electron local potential and $V^{(1)}(\mathbf{r})$ is the corresponding first order variation. The latter term

is due to the change in magnetisation density induced by $\boldsymbol{\mu}_K$. The perturbation does not give rise to a first order change in the charge density and so there is no change in the Hartree potential for linear order. This can be understood by considering the effect of time reversal; the charge density is even under time inversion, while the spin-magnetisation and magnetic field change sign. As a result the perturbation does not induce a first order change in the charge density, however there is a first order induced spin-magnetisation density. $V^{(1)}(\mathbf{r})$ therefore accounts for the first-order variation of the exchange-correlation term which we label as $H_{xc}^{(1)}$.

We now use the PAW transformation (Eqn. 3) to obtain the pseudo-Hamiltonian. As Eqn. 3 does not contain any field dependence it is sufficient to apply it to each term of Eqn. 4 individually. The pseudo-Hamiltonian at zeroth order in the perturbation is

$$\widetilde{H}^{(0)} = \frac{1}{2}\mathbf{p}^2 + V_{loc}(\mathbf{r}) + \sum_{\mathbf{R}} V_{nl}^{\mathbf{R}}, \quad (9)$$

where $V_{loc}(\mathbf{r})$ is the local part of the pseudopotentials which includes the self-consistent part of the Hamiltonian and $V_{nl}^{\mathbf{R}}$ is the non-local part which is given by $V_{nl}^{\mathbf{R}} = \sum_{n,m}|\widetilde{p}_{\mathbf{R},n}\rangle a_{n,m}^{\mathbf{R}}\langle\widetilde{p}_{\mathbf{R},n}|$. $a_{n,m}^{\mathbf{R}}$ are the strengths of the nonlocal potential in each channel at each ionic site. Collecting terms to linear order in the perturbation gives,

$$\widetilde{H}^{(1)} = \widetilde{H}_{xc}^{(1)} + \widetilde{H}_{SD} + \widetilde{H}_{FC}. \quad (10)$$

$\widetilde{H}_{SD}$ describes the spin-dipolar interaction induced by $\boldsymbol{\mu}_K$ and is given by

$$\widetilde{H}_{SD} = g\beta\mathbf{S} \cdot \mathbf{B}_K^{SD} + g\beta\mathbf{S} \cdot \Delta\mathbf{B}_K^{SD}. \quad (11)$$

The first term on the right-hand side is the all-electron operator and the second term is the augmentation to this,

$$\Delta\mathbf{B}_K^{SD} = \sum_{n,m}|\widetilde{p}_{\mathbf{R},n}\rangle\,[\,\langle\phi_{\mathbf{R},n}|\mathbf{B}_K^{SD}|\phi_{\mathbf{R},m}\rangle \quad (12)$$
$$-\langle\widetilde{\phi}_{\mathbf{R},n}|\mathbf{B}_K^{SD}|\widetilde{\phi}_{\mathbf{R},m}\rangle\,]\,\langle\widetilde{p}_{\mathbf{R},m}|,$$

with $\mathbf{R} = \mathbf{R}_K$. In Eqn. 11 we have only included the augmentation of the spin-dipolar operator at the site of the perturbing atom. This on-site approximation is fully justified given the localised nature of this operator.

$\widetilde{H}_{FC}$ is the Fermi-contact operator and can be constructed in a similar manner to the spin-dipole operator giving an all-electron and an augmentation contribution. However, as the Fermi-contact operator contains a Dirac delta-function and is therefore localised within the augmentation region, $\widetilde{H}_{FC}$ can be simplified considerably. The pseudo-partial waves and projectors, $\sum_n \langle\widetilde{p}_n|\widetilde{\phi}_n\rangle$, form a complete set which enables us to rewrite the all-electron contribution in terms of the pseudo-partial waves within the augmentation region and so we can equivalently express the operator as

$$\widetilde{H}_{FC} = g\beta\mathbf{S} \cdot \sum_{n,m}|\widetilde{p}_{\mathbf{R},n}\rangle\langle\phi_{\mathbf{R},n}|\mathbf{B}_K^{FC}|\phi_{\mathbf{R},m}\rangle\langle\widetilde{p}_{\mathbf{R},m}|, \quad (13)$$

where $\mathbf{R} = \mathbf{R}_K$. This form is more suitable for a practical calculation as it avoids an explicit representation of the delta-function.

B. Magnetisation Density

To construct the magnetisation density, we define $\mathbf{m}_i^{(1)}(\mathbf{r})$ to be the linear response to the magnetic field, $\mathbf{B}_i$ induced along the direction $\mathbf{u}_i$ by the spin-dipolar and Fermi-contact interactions. The total magnetisation density is obtained as $\mathbf{m}^{(1)} = \sum_{i=x,y,z} \mathbf{m}_i^{(1)}(\mathbf{r})$, the sum over the cartesian directions. By choosing $\mathbf{u}_i$ as the spin quantisation axis, $H^{(1)}$ is diagonal in the spin-up and spin-down basis. The eigenstates of $H^{(0)} + H^{(1)}$ are also eigenstates of $\mathbf{u}_i \cdot \mathbf{S}$ and so the magnetisation density is parallel to $\mathbf{u}_i$ giving;

$$\mathbf{m}_i^{(1)}(\mathbf{r}) = [\mathbf{u}_i \cdot \mathbf{m}_i^{(1)}(\mathbf{r})]\mathbf{u}_i = m_i^{(1)}(\mathbf{r})\mathbf{u}_i. \quad (14)$$

Here

$$m_i^{(1)}(\mathbf{r}) = g\beta \left[n_{i,\uparrow}^{(1)}(\mathbf{r}) - n_{i,\downarrow}^{(1)}(\mathbf{r}) \right] = 2g\beta n_{i,\uparrow}^{(1)}(\mathbf{r}), \quad (15)$$

where g and β were defined previously and $n_{i,\sigma}^{(1)}$ is the induced density for either spin-up or spin-down. The simplification of the magnetisation density in this way is a consequence of time reversal symmetry, namely the absence of a first-order charge density. This means that the spin-up and spin-down ground-state wavefunctions are equivalent, so that $|\widetilde{\psi}_{\uparrow o}^{(0)}\rangle = |\widetilde{\psi}_{\downarrow o}^{(0)}\rangle$. Also, the linear variation of the wavefunctions induced by the spin magnetisation are related through $|\widetilde{\psi}_{\uparrow o}^{(1)}\rangle = -|\widetilde{\psi}_{\downarrow o}^{(1)}\rangle$.

Within PAW, Eqn. 15 becomes

$$\begin{aligned}
m_i^{(1)}(\mathbf{r}) = & \; 4g\beta \mathrm{Re} \sum_o \langle \widetilde{\psi}_{\uparrow o}^{(1)}|\mathbf{r}\rangle\langle \mathbf{r}|\widetilde{\psi}_{\uparrow o}^{(0)}\rangle \\
& + \sum_{\mathbf{R},n,m} \langle \widetilde{\psi}_{o\uparrow}^{(1)}|\widetilde{p}_{\mathbf{R},n}\rangle \Big[\langle \phi_{\mathbf{R},n}|\mathbf{r}\rangle\langle \mathbf{r}|\phi_{\mathbf{R},m}\rangle \\
& - \langle \widetilde{\phi}_{\mathbf{R},n}|\mathbf{r}\rangle\langle \mathbf{r}|\widetilde{\phi}_{\mathbf{R},m}\rangle \Big] \langle \widetilde{p}_{\mathbf{R},n}|\widetilde{\psi}_{o\uparrow}^{(0)}\rangle. \quad (16)
\end{aligned}$$

Re signifies taking the real component, $|\widetilde{\psi}_{\uparrow o}^{(0)}\rangle$ are the eigenstates of the unperturbed Hamiltonian, $H^{(0)}$, $|\widetilde{\psi}_{\uparrow o}^{(1)}\rangle$ are the perturbed pseudowavefunctions and o indexes the occupied bands. The first term on the right hand side of Eqn. 16 is the pseudo-magnetisation density $\widetilde{m}_i^{(1)}$, and the second term is the corresponding augmentation. For simplicity, we drop the spin indexing on the ground-state wavefunctions from now on as the spin-dependence enters only through the perturbation.

To calculate $|\widetilde{\psi}_{\uparrow o}^{(1)}\rangle$ we employ a Green's function method where

$$|\widetilde{\psi}_{\uparrow o}^{(1)}\rangle = \mathcal{G}(\epsilon)|\psi_o^{(0)}\rangle = \sum_e \frac{|\psi_e^{(0)}\rangle\langle \psi_e^{(0)}|}{\epsilon_o - \epsilon_e} \widetilde{H}_i^{(1)}|\psi_o^{(0)}\rangle. \quad (17)$$

$\widetilde{H}_i^{(1)}$ is the first order Hamiltonian given by Eqn. 10 with the spin quantised along the $\mathbf{u}_i$ direction. $\mathcal{G}(\epsilon)$ is the Green's function, ϵ_o and ϵ_e are the eigenvalues of the occupied and empty bands. Rather than explicitly sum over the empty states, we project onto the occupied bands by multiplying Eqn. 17 through by $(\epsilon_o - \widetilde{H}^{(0)})$. We define $\mathcal{P} = \sum_e |\widetilde{\psi}_e^{(0)}\rangle\langle \widetilde{\psi}_e^{(0)}| = 1 - \sum_o |\widetilde{\psi}_o^{(0)}\rangle\langle \widetilde{\psi}_o^{(0)}|$ and rewrite Eqn. 17 as

$$(\epsilon_o - \widetilde{H}^{(0)})|\widetilde{\psi}_{\uparrow o}^{(1)}\rangle = \mathcal{P}\widetilde{H}_i^{(1)}|\widetilde{\psi}_o^{(0)}\rangle. \quad (18)$$

This is then solved using a conjugate gradient minimisation scheme, with an additional self-consistency condition to account for the dependence of $H_{xc}^{(1)}$ on the spin-density. For a more detailed account of this type of approach, see Ref. 39.

C. Induced Magnetic Field

The induced magnetic field at atom L, and subsequently the J-coupling between L and K, due to the spin magnetisation is obtained by combining Eqns. 1 and 16 to give

$$\mathbf{B}_{\mathbf{m}^{(1)}}^{(1)}(\mathbf{R}_L) = \widetilde{\mathbf{B}}_{SD}^{(1)}(\mathbf{R}_L) + \Delta\mathbf{B}_{SD}^{(1)}(\mathbf{R}_L) + \Delta\mathbf{B}_{FC}^{(1)}(\mathbf{R}_L), \quad (19)$$

where we have taken advantage of the linearity of Eqn. 1 to yield three separate terms. The first term is the pseudo spin-dipolar contribution and the second term is the spin-dipole augmentation. The notation used here implicitly assumes that a rotation over the spin-axis has been performed.

In practise, the pseudo-spin dipole term can be constructed from the Fourier transform of Eqn. 1,

$$\mathbf{B}_{SD}^{(1)}(\mathbf{G}) = -\frac{\mu_0}{3} \left[\frac{3(\widetilde{\mathbf{m}}^{(1)}(\mathbf{G}) \cdot \mathbf{G})\mathbf{G} - \widetilde{\mathbf{m}}^{(1)}(\mathbf{G})|\mathbf{G}|^2}{G^2} \right], \quad (20)$$

where $\widetilde{\mathbf{m}}^{(1)}(\mathbf{G})$ is the Fourier transform of the pseudo-magnetisation density and $\mathbf{G}$ is a reciprocal space lattice vector. The $G = 0$ term is neglected as the cell size is large compared with the strength of the perturbation which is small.

The induced magnetic field at atom L is then recovered by performing a slow inverse Fourier transform at the position of each responding nucleus. The spin dipole augmentation term is obtained by using an on-site approximation and evaluating terms of the form,

$$\Delta\mathbf{B}_{SD}^{(1)}(\mathbf{R}_L) = g\beta\frac{\mu_0}{2\pi}\mathrm{Re}\sum_{n,m}\langle \widetilde{\psi}_o^{(0)}|\Delta\mathbf{B}_L^{SD}|\widetilde{\psi}_{\uparrow o}^{(1)}\rangle. \quad (21)$$

$\Delta\mathbf{B}_L^{SD}$ is defined in Eqn. 12 but now the subscript indicates the responding rather than the perturbing nucleus. To evaluate this term and Eqn. 12, we note that $|\phi_n\rangle$ can be decomposed into the product of a radial ($|R_{nl}\rangle$) and an angular ($|Y_{lm}\rangle$) term. B_L^{SD} can also be rewritten as the

product of a radial and angular component such that the computation of the augmentation term involves the on-site calculation of $\langle R_{nl}|\frac{1}{r_L^3}|R_{n'l'}\rangle\langle Y_n|\frac{3\mathbf{r}_L\mathbf{r}_L^T}{r_L^2} - \mathcal{I}|Y_m\rangle$. The latter quantity reduces to an integral over spherical harmonics given by the Gaunt coefficients.

The Fermi-contact contribution, $\Delta\mathbf{B}_{FC}^{(1)}$, is obtained by following the same argument used in constructing $\widetilde{H}_{FC}$ (Eqn. 13) and is given by

$$\Delta\mathbf{B}_{FC}^{(1)}(\mathbf{R}_L) =$$
$$\frac{4\mu_0}{3}\mathrm{Re}\sum_{n,m}\langle\widetilde{\psi}_o^{(0)}|\widetilde{p}_{\mathbf{R},n}\rangle\langle\phi_{\mathbf{R},n}|\delta(\mathbf{r}_L)|\phi_{\mathbf{R},m}\rangle\langle\widetilde{p}_{\mathbf{R},m}|\widetilde{\psi}_{\uparrow o}^{(1)}\rangle,$$
$$(22)$$

which is the all-electron reconstruction of the induced magnetisation density at the responding nucleus.

IV. CURRENT DENSITY

We now obtain the contribution to the J-coupling tensor arising from the interaction of the nuclear spins mediated by the electron charge current. The derivation of the current density is similar to that of the magnetisation density and much of the notation is conserved throughout. We first obtain an expression for the pseudo-Hamiltonian in the presence of a perturbing nuclear spin and show how it can be used to obtain the induced current density. We then use this current density to calculate the magnetic field induced at the receiving nucleus.

A. Pseudo-Hamiltonian

The all-electron Hamiltonian for a system of N magnetic nuclei which interact through the nuclear vector potential, $\mathbf{A}(\mathbf{r}) = \sum_N \mathbf{A}_N(\mathbf{r}) = \frac{\mu_0}{4\pi}\sum_N\frac{\boldsymbol{\mu}_N\times\mathbf{r}_N}{|\mathbf{r}_N|^3}$, can be expanded to first order in $\boldsymbol{\mu}_K$ to give,

$$H_K = \frac{1}{2}\mathbf{p}^2 + V^{(0)}(\mathbf{r}) + H_{\mathbf{A}_K}, \qquad (23)$$

where

$$H_{\mathbf{A}_K} = \frac{\mu_0}{4\pi}\mathbf{p}\cdot\mathbf{A}_K(\mathbf{r}), \qquad (24)$$

and $V^{(0)}(\mathbf{r})$ is the ground-state local potential. The perturbation does not induce a first order change in either the charge or magnetisation densities and so unlike Eqn. 4, there is no linear variation to the self-consistent potential in Eqn. 23. We have used the symmetric gauge for the vector potential and taken the natural choice of gauge-origin; namely that for the Nth nuclear spin the gauge origin is the Nth atomic site giving $\mathbf{A}_N(\mathbf{r}) = 1/2\mathbf{B}(\mathbf{r})\times\mathbf{r}_N$. This gauge-choice preserves the translational invariance of the system and is much simpler than in the otherwise analogous case of NMR

chemical shielding. In the latter situation, due to the use of finite basis sets a rigid translation of the system in the uniform external magnetic field introduces an additional phase factor. For the planewave-pseudopotential approach the problem was solved by Pickard and Mauri with the development of the Gauge-Including Projector Augmented-Wave (GIPAW) approach, an extension which is unnecessary here.

To obtain the pseudo-Hamiltonian we now apply the PAW transformation of Eqn. 3 to Eqn. 23. The zeroth order term is again given by Eqn. 9 and the first order term by

$$\widetilde{H}_{\mathbf{A}_K} = \frac{\mu_0}{4\pi}\boldsymbol{\mu}_K\cdot\frac{\mathbf{r}_K\times\mathbf{p}}{|\mathbf{r}_K|^3} +$$
$$\frac{\mu_0}{4\pi}\boldsymbol{\mu}_K\cdot\sum_{n,m}|\widetilde{p}_{\mathbf{R},n}\rangle\left[\langle\phi_{\mathbf{R},n}|\frac{\mathbf{L}_K}{|\mathbf{r}_K|^3}|\phi_{\mathbf{R},m}\rangle\right.$$
$$\left.- \langle\widetilde{\phi}_{\mathbf{R},n}|\frac{\mathbf{L}_K}{|\mathbf{r}_K|^3}|\widetilde{\phi}_{\mathbf{R},m}\rangle\right]\langle\widetilde{p}_{\mathbf{R},m}|. \qquad (25)$$

The first term on the right-hand side is the all-electron component and the second term is the augmentation which is constructed at the site of the perturbing nucleus. $\mathbf{L}_K = \mathbf{r}_K\times\mathbf{p}$ is the angular momentum operator centred on the perturbing atomic site.

B. Current Density

The current density operator, $\mathbf{J}(\mathbf{r})$, is given by the sum of a paramagnetic and a diamagnetic term,

$$\mathbf{J}(\mathbf{r}) = \mathbf{J}^p(\mathbf{r}) + \mathbf{J}^d(\mathbf{r}), \qquad (26)$$

where the paramagnetic term is given by

$$\mathbf{J}^p(\mathbf{r}) = -\left[\mathbf{p}|\mathbf{r}\rangle\langle\mathbf{r}| + |\mathbf{r}\rangle\langle\mathbf{r}|\mathbf{p}\right]/2, \qquad (27)$$

and the diamagnetic term is

$$\mathbf{J}^d(\mathbf{r}) = -\mathbf{A}(\mathbf{r})|\mathbf{r}\rangle\langle\mathbf{r}|. \qquad (28)$$

If we consider the current due only to the perturbing nucleus, and with our atomic choice of gauge origin, the diamagnetic term can be written as

$$\mathbf{J}_K^d(\mathbf{r}) = -\frac{\mu_0}{4\pi}\frac{\boldsymbol{\mu}_K\times\mathbf{r}_K}{r_K^3}|\mathbf{r}\rangle\langle\mathbf{r}|. \qquad (29)$$

By applying Eqn. 3 to both Eqns. 27 and 29, we obtain the pseudo-current density operator within PAW

$$\widetilde{\mathbf{J}}(\mathbf{r}) = \mathbf{J}^p(\mathbf{r}) + \mathbf{J}_K^d(\mathbf{r}) + \left[\Delta\mathbf{J}^p(\mathbf{r}) + \Delta\mathbf{J}_K^d(\mathbf{r})\right], \qquad (30)$$

where the paramagnetic augmentation operator is

$$\Delta\mathbf{J}^p(\mathbf{r}) = \sum_{\mathbf{R},n,m}|\widetilde{p}_{\mathbf{R},n}\rangle\left[\langle\phi_{\mathbf{R},n}|\mathbf{J}^p|\phi_{\mathbf{R},m}\rangle\right.$$
$$\left.- \langle\widetilde{\phi}_{\mathbf{R},n}|\mathbf{J}^p|\widetilde{\phi}_{\mathbf{R},m}\rangle\right]\langle\widetilde{p}_{\mathbf{R},m}|, \qquad (31)$$

and the corresponding diamagnetic operator is

$$\Delta \mathbf{J}_{\mathrm{K}}^{\mathrm{d}}(\mathbf{r}) = \sum_{\mathbf{R},n,m} |\widetilde{p}_{\mathbf{R},n}\rangle \left[\langle \phi_{\mathbf{R},n}|\mathbf{J}_{\mathrm{K}}^{\mathrm{d}}|\phi_{\mathbf{R},m}\rangle \right.$$
$$\left. - \langle \widetilde{\phi}_{\mathbf{R},n}|\mathbf{J}_{\mathrm{K}}^{\mathrm{d}}|\widetilde{\phi}_{\mathbf{R},m}\rangle \right] \langle \widetilde{p}_{\mathbf{R},m}|. \quad (32)$$

Arranging terms in $\mathbf{J}(\mathbf{r})$ to zeroth and linear order in $\boldsymbol{\mu}_{\mathrm{K}}$ gives

$$\mathbf{J}^{(0)}(\mathbf{r}) = \mathbf{J}^{\mathrm{p}}(\mathbf{r}) + \Delta \mathbf{J}^{\mathrm{p}}(\mathbf{r}), \quad (33)$$

and

$$\mathbf{J}^{(1)}(\mathbf{r}) = \mathbf{J}_{\mathrm{K}}^{\mathrm{d}}(\mathbf{r}) + \Delta \mathbf{J}_{\mathrm{K}}^{\mathrm{d}}(\mathbf{r}). \quad (34)$$

Using Eqns. 33 and 34 we are now able to obtain the first-order induced current density, which within density functional perturbation theory is given by

$$\mathbf{j}^{(1)}(\mathbf{r}) = 2\sum_{o} 2\,\mathrm{Re}\langle \widetilde{\psi}_{o}^{(0)}|\widetilde{\mathbf{J}}^{(0)}|\widetilde{\psi}_{o}^{(1)}\rangle + \langle \widetilde{\psi}_{o}^{(0)}|\widetilde{\mathbf{J}}^{(1)}|\widetilde{\psi}_{o}^{(0)}\rangle,$$
$$= \mathbf{j}_{\mathrm{p}}^{(1)}(\mathbf{r}) + \mathbf{j}_{\mathrm{d}}^{(1)}(\mathbf{r}). \quad (35)$$

Here $|\widetilde{\psi}_{o}^{(0)}\rangle$ is the unperturbed wavefunction, $|\widetilde{\psi}_{o}^{(1)}\rangle$ is the perturbed wavefunction and o indexes the occupied bands. The first term on the right hand side is the paramagnetic contribution to the induced current and the second term is the diamagnetic contribution. The first order wavefunction is again obtained using Eqn. 18 where $\widetilde{\mathrm{H}}^{(1)}$ is now given by Eqn. 25.

C.   Induced Magnetic Field

We can now combine Eqns. 1 and 35 to calculate the J-coupling between nuclei L and K arising from the magnetic field induced by the orbital current. The magnetic field at nucleus L due to the orbital current can be expressed as the sum of 4 terms,

$$\mathbf{B}_{\mathbf{j}^{(1)}}^{(1)}(\mathbf{R}_{\mathrm{L}}) = \widetilde{\mathbf{B}}_{\mathrm{p}}^{(1)}(\mathbf{R}_{\mathrm{L}}) + \widetilde{\mathbf{B}}_{\mathrm{d}}^{(1)}(\mathbf{R}_{\mathrm{L}}) + \Delta \mathbf{B}_{\mathrm{p}}^{(1)}(\mathbf{R}_{\mathrm{L}})$$
$$+ \Delta \mathbf{B}_{\mathrm{d}}^{(1)}(\mathbf{R}_{\mathrm{L}}), \quad (36)$$

the pseudised contributions from the paramagnetic and diamagnetic currents and their respective augmentation terms.

To calculate the pseudised contributions to the current density we obtain the Fourier transform of $\widetilde{\mathbf{B}}_{\mathrm{p}}^{(1)}(\mathbf{R}_{\mathrm{L}})$ and $\widetilde{\mathbf{B}}_{\mathrm{d}}^{(1)}(\mathbf{R}_{\mathrm{L}})$ giving

$$\mathbf{B}^{(1)}(\mathbf{G}) = \mu_0 \frac{i\mathbf{G} \times \mathbf{j}_{\mathrm{p/d}}^{(1)}(\mathbf{G})}{G^2}, \quad (37)$$

where $\mathbf{j}_{\mathrm{p/d}}^{(1)}(\mathbf{G})$ is the Fourier transform of either the paramagnetic or diamagnetic current. To obtain the induced

field at the atom site L we perform a slow Fourier transform of Eqn. 37. We again note that the G=0 contribution to $\mathbf{B}^{(1)}(\mathbf{G})$ is neglected as the contribution is expected to be small. The augmentation to the paramagnetic current is calculated using an on-site approximation ($\mathbf{R} = \mathbf{R}_{\mathrm{L}}$) with

$$\Delta \mathbf{B}_{\mathrm{p}}^{(1)}(\mathbf{R}_{\mathrm{L}}) = \frac{\mu_0}{4\pi}\sum_{n,m} \langle \widetilde{\psi}_{o}^{(0)}|\widetilde{p}_{\mathbf{R},n}\rangle \left[\langle \phi_{\mathbf{R},n}|\frac{\mathbf{L}_{\mathrm{L}}}{\mathbf{r}_{\mathrm{L}}^3}|\phi_{\mathbf{R},m}\rangle \right.$$
$$\left. - \langle \widetilde{\phi}_{\mathbf{R},n}|\frac{\mathbf{L}_{\mathrm{L}}}{\mathbf{r}_{\mathrm{L}}^3}|\widetilde{\phi}_{\mathbf{R},m}\rangle \right] \langle \widetilde{p}_{\mathbf{R},m}|\widetilde{\psi}_{o}^{(1)}\rangle, \quad (38)$$

where $\mathbf{L}$ is the angular momentum operator evaluated with respect to the augmentation regions. The augmentation to the diamagnetic current is given by

$$\Delta \mathbf{B}_{\mathrm{d}}^{(1)} = \frac{\mu_0}{4\pi}\sum_{\mathbf{R},n,m} \langle \widetilde{\psi}_{o}^{(0)}|\widetilde{p}_{\mathbf{R},n}\rangle$$
$$\left[\langle \phi_{\mathbf{R},n}|\frac{r_{\mathrm{L}}r_{\mathrm{K}} - \mathbf{r}_{\mathrm{L}}\mathbf{r}_{\mathrm{K}}^{\mathrm{T}}}{r_{\mathrm{L}}^3 r_{\mathrm{K}}^3}|\phi_m\rangle \right.$$
$$\left. - \langle \widetilde{\phi}_{\mathbf{R},n}|\frac{r_{\mathrm{L}}r_{\mathrm{K}} - \mathbf{r}_{\mathrm{L}}\mathbf{r}_{\mathrm{K}}^{\mathrm{T}}}{r_{\mathrm{L}}^3 r_{\mathrm{K}}^3}|\widetilde{\phi}_m\rangle \right] \langle \widetilde{p}_{\mathbf{R},m}|\widetilde{\psi}_{o}^{(1)}\rangle. \quad (39)$$

This is much more difficult to evaluate than any other term as an on-site approximation cannot be used due to the presence of the $\mathbf{r}_{\mathrm{K}}$ position vector within the augmentation summation. However, previous quantum chemical studies have shown that the overall contribution to the J-coupling from the diamagnetic term is very small compared with any of the other three contributions. In light of this, we have neglected this term in our current implementation.

V.   RESULTS

We have implemented our theory into a parallelised plane-wave electronic structure code.[40] The ground-state wavefunctions and Hamiltonian are obtained self-consistently after which the isotropic J-coupling constant is calculated using the outlined approach. In our implementation we use norm-conserving Troullier-Martins pseudopotentials.[41] For the all-electron reconstruction we used two projectors per angular momentum channel.

In the following sections we compare our approach to existing quantum chemistry approaches which use localised basis sets and with experiment.

A.   Molecules

To validate our method we have calculated isotropic coupling constants for a range of small molecules[42] and compared them with experiment. There are several
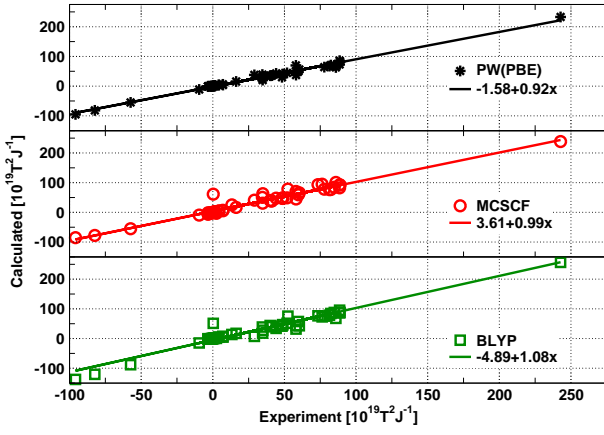
FIG. 2: J-couplings calculated for a set of molecules. Both the MCSCF and BLYP results were taken from Ref. 43. All of the experimental values were also taken from this paper. The PW(PBE) results are from the present work. The lines are obtained from a linear regression of the calculated values with experiment. All values are quoted in $10^{19}T^2J^{-1}$, the unit of the reduced coupling constant.

studies of calculated J-couplings for small molecules reported in the literature, using a variety of theoretical approaches, see Ref. 14 and references therein. We compare our results to calculations presented by Lantto *et al*[43] which were obtained within DFT using the BLYP functional and with the Multi-configurational Self-Consistent Field (MCSCF) approach. For consistency we use the molecular geometries reported in their work.

To obtain the isotropic J-coupling we use a supercell of size 1728 $Å^3$ for each molecule with the exception of benzene which required a larger cell-size of 3375 $Å^3$. The exchange-correlation was approximated by GGA-PBE[44] and an energy cut-off of 80 Ry was imposed on the planewave expansion. All calculations sample the Brillouin zone at the gamma-point and used norm-conserving Trouillier-Martins pseudopotentials.[41] The calculated J-coupling against experiment for the molecules are shown in Fig. 2 alongside the results of a linear regression for each set of data. These results are presented as reduced spin-coupling constants, which are given by $\overleftrightarrow{\mathbf{K}}_{LK} = \frac{2\pi \overleftrightarrow{\mathbf{J}}_{LK}}{\hbar \gamma_L \gamma_K}$, and so are independent of nuclear species. The graph indicates an excellent overall agreement with both experiment and the other approaches. The accuracy of the planewave PBE calculations is comparable with the all-electron BLYP results, with regression coefficients of 0.92 and 1.08 respectively. The correlation coefficients for the BLYP, MCSCF and PW data are 0.97, 0.97 and 0.99 respectively, suggesting a smaller random error in the planewave approach. Unsurprisingly, the most accurate couplings are given by MCSCF, which provides a more comprehensive description of electron correlation but is computationally more demanding than DFT.

In Table I we present the J-coupling values calculated for benzene. The results compare favourably with

TABLE I: J-coupling[Hz] in benzene. PW(PBE) labels the current planewave approach. The BLYP, MCSCF and experimental values were taken from Ref. 43. D, P, FC and SD label the diamagnetic, paramagnetic, Fermi-contact and spin-dipolar contributions respectively. All values are in Hz.

J_{KL}^n	Method	D	P	FC	SD	Total	Expt[Hz]
J_{CC}^1	PW(PBE)	0.2	−6.9	58.2	1.9	53.4	55.8
	BLYP	0.2	−6.8	63.8	1.0	58.2	
	MCSCF	0.4	−6.6	75.1	1.5	70.9	
J_{CC}^2	PW(PBE)	0.0	0.0	−1.2	−0.3	−1.5	−2.5
	BLYP	0.0	0.1	0.0	−0.5	−0.4	
	MCSCF	−0.2	0.0	−3.7	−1.1	−5.0	
J_{CC}^3	PW(PBE)	0.0	0.6	7.3	1.1	9.0	10.1
	BLYP	0.0	0.5	8.4	1.5	10.4	
	MCSCF	0.1	0.4	16.8	1.8	19.1	
J_{CH}^1	PW(PBE)	0.5	0.9	132.5	−0.2	133.7	158.3
	BLYP					155.2	
	MCSCF					185.1	
J_{CH}^2	PW(PBE)	−0.1	0.2	5.1	0.1	5.3	1.0
	BLYP					1.1	
	MCSCF					−9.8	
J_{CH}^3	PW(PBE)	−0.2	−1.1	6.0	0.0	4.7	7.6
	BLYP					7.4	
	MCSCF					12.9	
J_{CH}^4	PW(PBE)	−0.1	0.3	−0.4	0.0	−0.2	−1.2
	BLYP					−1.3	
	MCSCF					−6.1	

both the existing approaches and with experiment. The MCSCF approach systematically overestimates the J-coupling for both J_{CH} and J_{CC} compared with experiment. This is due to the use of a restricted basis set which was necessary given the size of the system, for further details see Ref. 45.

The decomposition of the J-coupling into the four components serves as an illustration of the relative strengths of each contribution and the trends over several bonds. Lantto *et al* have only presented this separation for J_{CC}. It is clear that the Fermi-contact is the dominant mechanism in the coupling and that the diamagnetic component is consistently the smallest and is often negligible.

B. Crystals

Due to the difficulties encountered measuring J-coupling in solid-state systems there are very few values to be found in the literature that are suitable for validation of our approach. Recently Coelho *et al.*[4] provided an estimate for the two bond coupling between ^{29}Si and ^{31}P pairs in the silicophosphate $Si_5O(PO_4)_6$. Subsequently this was followed by a more accurate determination[6] which identified the four Si-O-P couplings. We have calculated NMR chemical shifts and J_{P-O-Si}^2 for $Si_5O(PO_4)_6$ to validate our approach.

The structure of $Si_5O(PO_4)_6$ is trigonal (a=7.869Å, c=24.138Å, 36 atoms per primitive cell) and contains

TABLE II: Calculated J-coupling for silicophosphate $Si_5O(PO_4)_6$ using the unit cell and two supercells constructed with $2\times1\times1$ and $2\times2\times1$ unit cells.

Coupling	$1\times1\times1$	$2\times1\times1$	$2\times2\times1$
$^2J_{P-O_3-Si_1}$	-17.37	-17.07	-17.12
$^2J_{P-O_2-Si_2}$	-16.16	-16.18	-16.26
$^2J_{P-O_5-Si_2}$	-1.30	-1.20	-1.17
$^2J_{P-O_4-Si_3}$	-13.83	-14.18	-14.13

TABLE III: Calculated NMR chemical shifts[47] and J-coupling for silicophosphate $Si_5O(PO_4)_6$. The experimental values are in brackets and were taken from Ref. 6.

Coupling	^{31}P [ppm]	^{29}Si [ppm]	Calc. [Hz]
$J^2_{P-O_3-Si_1}$	-47.4 (-43.8)	-214.8 (-213.3)	-17.12 (15±2)
$J^2_{P-O_2-Si_2}$		-218.7 (-217.0)	-16.26 (14±2)
$J^2_{P-O_5-Si_2}$		-218.7 (-217.0)	-1.17 (4±2)
$J^2_{P-O_4-Si_3}$		-128.6 (-119.1)	-14.13 (12±2)

TABLE IV: Decomposition for the J-coupling in $Si_5O(PO_4)_6$. D is the diamagnetic term, P is the paramagnetic term, SD is the spin-dipolar and FC is the Fermi-contact.

Coupling	D	P	SD	FC	Total
$^2J_{P-O_3-Si_1}$	-0.05	-0.27	-0.03	-16.77	-17.12
$^2J_{P-O_2-Si_2}$	-0.02	-0.50	-0.23	-15.51	-16.26
$^2J_{P-O_5-Si_2}$	-0.10	-0.07	0.18	-1.18	-1.17
$^2J_{P-O_4-Si_3}$	-0.09	-0.49	0.23	-13.79	-14.13

one unique P site and three inequivalent Si sites. Two of these Si sites are 6-fold coordinated, Si_1 and Si_2, and the third site, Si_3, is four-fold coordinated. Si_1 is bonded to six equivalent oxygen atoms, Si_2 is bonded to six oxygen atoms which are comprised of two distinct sites. Si_3 is bonded to three equivalent oxygen atoms and one oxygen from an Si_3-O tetrahedron. Thus there is one ^{31}P chemical shift, three ^{29}Si chemical shifts and four unique $^2J_{P-O-Si}$ couplings.

We obtained the structure from the Chemical Database Service at Daresbury.[46] Prior to calculating the NMR parameters, we performed a full geometry optimisation on the structure, using a planewave cut-off of 70 Ryd and norm-conserving pseudopotentials. The GGA-PBE[44] exchange-correlation functional was used and a Monkhorst-Pack k-point grid with a maximum of 0.1 $Å^{-1}$ between sampling points. We calculated the NMR chemical shifts using the GIPAW[21] approach with the same parameters used for the geometry optimisation. The J-coupling between P and Si was obtained using the approach outlined above. A slightly higher maximum planewave energy (80Ryd) was required to give J-couplings converged to within 0.1Hz.

We tested the convergence of the induced magnetization density and current density with respect to supercell size. The results of these calculations for three cell sizes are presented in table II. From this we can see that both the induced magnetization and current densities have decayed substantially within the single unit cell. The largest of these calculations (144 atoms) was parallelised over 16 dual-core AMD processors and took 45 hours to run. The groundstate calculation took approximately 14 hours and the J-coupling terms; Fermi-contact, spin-dipolar and orbital, required 3.5 hours, 15.5 hours and 11.4 hours respectively.

The results for the $2\times2\times1$ cells are presented in comparison with experiment in Table III. From Table III it is clear that the calculated J-couplings are in excellent agreement with experiment and fully reproduce the surprisingly large spread in the J-coupling values. Our calculations verify the novel experimental work and also identify the sign of the couplings which are not determined by the experimental spin-echo based approaches.

The NMR chemical shifts are also in good agreement with experiment, particularly for ^{29}Si. For both ^{29}Si and ^{31}P the difference between the calculated and experimental values is a very small fraction of the total

shift range. We note that our assignment of the three Si sites in $Si_5O(PO_4)_6$ agrees with the assignment based on experimental intensities as discussed by Coelho *et al*[4]. In Table IV we present the decomposition of the silicophosphate J-coupling into their constituent terms. As with benzene, the Fermi-contact is found to be consistently the largest component while the diamagnetic and spin-dipolar contributions are very small.

VI. CONCLUSIONS

We have developed an all-electron approach for calculating NMR J-coupling constants using planewaves and pseudopotentials within DFT. Our method is applicable to both solution and solid state systems using supercell techniques. We have validated our theory against existing quantum chemical approaches and experiment for molecules. We have calculated the J-coupling between Si and P in a silicophosphate polymorph, for which we have determined the sign of the coupling.

Given the recent experimental interest in J-coupling, we expect that our approach will prove useful in determining both the range and strength of coupling in systems not yet investigated and whether or not such couplings can feasibly be determined by experiment. By combining J-coupling calculations with computations of other NMR parameters, there now exists a comprehensive set of computational tools to complement experimental understanding and design.

VII. ACKNOWLEDGMENTS

[1] M. H. Levitt, *Spin Dynamics. Basics of Nuclear Magnetic Resonance* (Wiley, 2001).

[2] L. Duma, W. C. Lai, M. Carravetta, L. Emsley, S. P. Brown, and M. H. Levitt, ChemPhysChem **5**, 815 (2004).

[3] J. P. Amoureux, J. Trebosc, J. W. Wiench, D. Massiot, and M. Pruski, Solid State Nucl. Magn. Reson. **27**, 228 (2005).

[4] C. Coelho, T. Azais, L. Bonhomme-Coury, J. Maquet, D. Massiot, and C. Bonhomme, J. Mag. Res. **179**, 114 (2006).

[5] S. Cadars, A. Lesage, M. Trierweiler, L. Heux, and L. Emsley, Phys. Chem. Chem. Phys. **9**, 92 (2007).

[6] C. Coelho, T. Azais, L. Bonhomme-Coury, G. Laurent, and C. Bonhomme, Inorg. Chem. **46**, 1379 (2007).

[7] S. P. Brown, M. Perez-Torralba, D. Sanz, R. M. Claramunt, and L. Emsley, Chem. Commun. pp. 1852–1853 (2002).

[8] S. P. Brown, M. Perez-Torralba, D. Sanz, R. M. Claramunt, and L. Emsley, J. Am. Chem. Soc. **124**, 1152 (2002).

[9] W. C. Lai, N. McLean, A. Gansmuller, M. A. Verhoeven, G. C. Antonioli, M. Carravetta, L. Duma, P. H. M. Bovee-Geurts, O. G. Johannessen, H. J. M. de Groot, et al., J. Am. Chem. Soc. **128**, 3878 (2006).

[10] S. P. Brown and L. Emsley, J. Magn. Reson. **171**, 43 (2004).

[11] T. N. Pham, J. M. Griffin, S. Masiero, S. Leno, G. Gottarelli, P. Hodgkinson, C. Filip, and S. P. Brown, Phys. Chem. Chem. Phys. **9**, 3416 (2007).

[12] A. J. Dingley and S. Grzesiek, J. Am. Chem. Soc **120**, 8293 (1998).

[13] A. J. Dingley, R. D. Peterson, S. Grzesiek, and J. Feigon, J. Am. Chem. Soc. **127**, 14466 (2005).

[14] J. Vaara, J. Jokisaari, R. E. Wasylishen, and D. L. Bryce, Prog. Nucl. Magn. Reson. Spectrosc. **41**, 233 (2002).

[15] T. Helgaker, M. Jaszunski, and K. Ruud, Chem. Rev. **99**, 293 (1999).

[16] M. Kaupp, M. Bühl, and V. G. Malkin, eds., *Calculation of NMR and EPR Parameters. Theory and Applications* (Wiley VCH, Weinheim, 2004).

[17] S. Grzesiek, F. Cordier, V. Jaravine, and M. Barfield, Prog. Nucl. Magn. Reson. Spectrosc. **45**, 275 (2004).

[18] J. C. Facelli and D. M. Grant, Nature **365**, 325 (1993).

[19] C. Ochsenfeld, S. P. Brown, I. Schnell, J. Gauss, and H. W. Spiess, J. Am. Chem. Soc. **123**, 2597 (2001).

[20] R. Salzmann, C. J. Ziegler, N. Godbout, M. T. McMahon, K. S. Suslick, and E. Oldfield, J. Am. Chem. Soc. **120**, 11323 (1998).

[21] C. J. Pickard and F. Mauri, Phys. Rev. B **63**, 245101 (2001).

[22] M. C. Payne, M. P. Teter, D. C. Allen, T. A. Arias, and J. D. Joannopoulos, Rev. Mod. Phys. **64**, 1045 (1992).

[23] S. E. Ashbrook, L. L. Polles, R. Gautier, C. J. Pickard, and R. I. Walton, Phys. Chem. Chem. Phys. **8**, 3423 (2006).

[24] I. Farnan, E. Balan, C. J. Pickard, and F. Mauri, Am. Miner. **88**, 1663 (2003).

[25] M. Profeta, F. Mauri, and C. J. Pickard, J. Am. Chem. Soc. **125**, 541 (2003).

[26] M. Benoit, M. Profeta, F. Mauri, C. J. Pickard, and M. E. Tuckerman, J. Phys. Chem. B **109**, 6052 (2005).

[27] T. Charpentier, S. Ispas, M. Profeta, F. Mauri, and C. J. Pickard, J. Phys. Chem. B **108**, 4147 (2004).

[28] J. R. Yates, C. J. Pickard, M. C. Payne, R. Dupree, M. Profeta, and F. Mauri, J. Phys. Chem. A **108**, 6032 (2004).

[29] C. Gervais, R. Dupree, K. J. Pike, C. Bonhomme, M. Profeta, C. J. Pickard, and F. Mauri, J. Phys. Chem. A **109**, 6960 (2005).

[30] J. R. Yates, T. N. Pham, C. J. Pickard, F. Mauri, A. M. Amado, A. M. Gil, and S. P. Brown, J. Am. Chem. Soc. **127**, 10216 (2005).

[31] P. E. Blöchl, Phys. Rev. B **50**, 17 953 (1994).

[32] N. F. Ramsey and E. M. Purcell, Phys. Rev. **85**, 143 (1952).

[33] N. F. Ramsey, Phys. Rev. **91**, 303 (1953).

[34] B. L. Marquez, W. H. Gerwick, and R. T. Willianson, Magn. Reson. Chem. **39**, 449 (2001).

[35] R. A. E. Edden and J. Keeler, J. Mag. Res. **166**, 53 (2004).

[36] C. G. van de Walle and P. E. Blöchl, Phys. Rev. B **47**, 4244 (1993).

[37] H. M. Petrilli, P. E. Blöchl, P. Blaha, and K. Schwarz, Phys. Rev. B **57**, 14690 (1998).

[38] C. J. Pickard and M. C. Payne, Inst. Phys. Conf. Ser. **153**, 179 (1997).

[39] X. Gonze, Phys. Rev. B **55**, 10337 (1995).

[40] S. J. Clark, M. D. Segall, C. J. Pickard, P. J. Hasnip, M. J. Probert, K. Refson, and M. C. Payne, Z. Kristall. **220**, 567 (2005).

[41] N. Troullier and J. L. Martins, Phys. Rev. B **43**, 1993 (1991).

[42] C_2H_2, C_2H_4, C_2H_6, C_6H_6, HCN, HNC, CH_3CN, CH_3NC, CH_3F, CHF_3, OF_2, CH_3SiH_3, HF, HCl, H_2O, CH_4, SiH_4.

[43] P. Lantto, J. Vaara, and T. Helgaker, J. Chem. Phys **117**, 5998 (2002).

[44] J. P. Perdew, K. Burke, and M. Ernzerhof, Phys. Rev. Lett. **77**, 3865 (1996).

[45] J. Kaski, J. Vaara, and J. Jokisaari, J. Am. Chem. Soc. **118**, 8879 (1996).

[46] D. Fletcher, R. McMeeking, and D. Parkin, J. Chem. Inf. Comput. Sci. **36**, 746 (1996).

[47] The reference shieldings required to convert the calculated shieldings into chemical shifts were obtained from Ref. 25 for Si and Ref. 48 for P.

[48] M. Profeta, M. Benoit, F. Mauri, and C. J. Pickard, J. Am. Chem. Soc. **126**, 12628 (2004).